

# Imaging of the Internal Nasal Valve Using Long-Range Fourier Domain Optical Coherence Tomography

Anna S. Englhard, MD; Maximilian Wiedmann, MS; Georg J. Ledderose, MD; Bryan Lemieux, BS;  
Alan Badran, BS; Zhongping Chen, PhD; Christian S. Betz, MD; Brian J. Wong, MD, PhD

**Objectives/Hypothesis:** To evaluate for the first time the feasibility and methodology of long-range Fourier domain optical coherence tomography (LR-OCT) imaging of the internal nasal valve (INV) area in healthy individuals.

**Study Design:** Prospective individual cohort study.

**Methods:** For 16 individuals, OCT was performed in each nare. The angle and the cross-sectional area of the INV were measured. OCT images were compared to corresponding digital pictures recorded with a flexible endoscope.

**Results:** INV angle measured by OCT was found to be  $18.3^\circ \pm 3.1^\circ$  (mean  $\pm$  standard deviation). The cross-sectional area was  $0.65 \pm 0.23 \text{ cm}^2$ . The INV angle measured by endoscopy was  $18.8^\circ \pm 6.9^\circ$ . There was no statistically significant difference between endoscopy and OCT concerning the mean INV angle ( $P = .778$ ), but there was a significant difference in test precision (coefficient of variance 50% vs. 15%;  $P < .001$ ).

**Conclusions:** LR-OCT proved to be a fast and easily performed method. OCT could accurately quantify the INV area. The values of the angle and the cross-sectional area of the INV were reproducible and correlated well with the data seen with other methods. Changes in size could be reliably delineated. Endoscopy showed similar values but was significantly less precise.

**Key Words:** Optical coherence tomography, internal nasal valve, nasal obstruction, endoscopy, long-range Fourier domain.

**Level of Evidence:** 2b.

*Laryngoscope*, 00:000–000, 2015

## INTRODUCTION

An often overlooked cause of nasal airway obstruction is collapse or obstruction of the internal nasal valve (INV).<sup>1,2</sup> It is the narrowest part of the nasal airway and therefore the point where resistance to flow is greatest.<sup>1</sup> It is located approximately 1.3 cm from the nares and is bounded medially by the septum, laterally by the upper lateral cartilages, and inferiorly by the anterior end of the inferior turbinate and the floor of the nose.<sup>3</sup> The INV is a slit-like opening with a cross-sectional area of about 55 to 65 mm.<sup>4–6</sup> In asymptomatic, normal subjects, an angle of about 10 to 15° exists between the upper lateral cartilage and the septum.<sup>2,7,8</sup> An INV may collapse when this angle is less than these values. Even minor

changes to the geometry of the nasal valve region may have a significant impact on nasal airflow. The etiology can be congenital, traumatic, or iatrogenic.<sup>8</sup> Improving or correcting the nasal valve area/angle has been an active area of interest for surgeons who perform functional rhinoplasty.<sup>9</sup>

Currently, there is no gold standard test to diagnose INV obstruction.<sup>3</sup> History and physical examination, including anterior rhinoscopy and the Cottle maneuver, are key measures for distinguishing among septal, turbinate, and sidewall causes.<sup>10–12</sup> Nasal endoscopy is the only widely accepted adjunct test for examining the nasal valve area.<sup>3,10</sup> However, all of these methods are subject to broad examiner variability and therefore lack objectivity. Classic rhinomanometry and acoustic rhinometry have been described to assess nasal resistance and the cross-sectional area of the nasal valve region.<sup>4,5,13</sup> However, several limitations, including high costs and lack of reliability, have led to limited use.<sup>1,10,11</sup> Computed tomography (CT) has been proposed as an objective tool to provide anatomical information,<sup>14–17</sup> but currently, there are no data to show that radiographic studies are useful in evaluating the extent of nasal valve collapse.<sup>3,10</sup> CT is not commonly ordered for nasal airway obstruction management alone.<sup>18</sup>

Optical coherence tomography (OCT) is a minimally invasive imaging modality that combines nonionizing near infrared light with principles of low coherence interferometry.<sup>19</sup> It acquires high-resolution (10  $\mu\text{m}$ ),

From the Department of Otolaryngology–Head and Neck Surgery, Ludwig Maximilian University Munich, Munich, Germany (A.S.E., G.J.L., C.S.B.); and Department of Biomedical Engineering (M.W., Z.C.), Beckman Laser Institute (B.L., A.B., B.J.W.); and the Department of Otolaryngology–Head and Neck Surgery (B.J.W.), University of California, Irvine, Irvine, California, U.S.A.

Editor's Note: This Manuscript was accepted for publication October 26, 2015.

First results of this study were presented at the 86th Annual Meeting of the German Society of Oto-Rhino-Laryngology, Head and Neck Surgery, Berlin, Germany, May 14–16, 2015.

The authors have no funding, financial relationships, or conflicts of interest to disclose.

Send correspondence to Brian J. Wong, Department of Otolaryngology–Head and Neck Surgery, University of California, Irvine, Orange, CA 92868. E-mail: bjwong@uci.edu

DOI: 10.1002/lary.25785

cross-sectional images in turbid media such as living tissue. OCT has been widely used in ophthalmology to image the retina and in cardiovascular applications to image vulnerable plaque in the coronary vasculature. Clinically, in the head and neck, OCT has primarily been used to image tissue structure with a focus on examining cancer and neoplasia. However, our group and others have used a variant of conventional OCT, long-range OCT (LR-OCT), as an optical rangefinder.<sup>20,21</sup> LR-OCT provides a means to measure the structural anatomy of large hollow organs such as the upper airway, and to generate reliable models.

Previous studies using LR-OCT demonstrated the capability of OCT to acquire anatomic and substructural images of the human upper airway, and generate volumetric representations of the upper airway.<sup>21,22</sup> The objective of this study was to evaluate for the first time the feasibility and methodology of LR-OCT imaging of the nasal valve area in normal individuals.

## MATERIALS AND METHODS

### *Study Design*

Approval for this study was obtained from the institutional review board at the University of California, Irvine. Informed consent was obtained from all subjects. No compensation was provided. We conducted a prospective study to evaluate LR-OCT for the measurement of the INV in 16 healthy subjects without complaints of recurrent sinusitis, nasal airway obstruction, allergies, or previous operation on the nose. For each individual, OCT was performed in each nare. The angle and the cross-sectional area of the INV were measured. OCT images were compared to corresponding digital images recorded with a conventional flexible endoscope.

### *Endoscopic Measurement*

Before starting OCT imaging, all 16 subjects underwent bilateral endoscopic evaluation of the nasal airway. The endoscope was inserted through the nostril until the INV was visible. Three different videos and separate still images of the nasal valve were recorded. The procedure was repeated 5 minutes after the application of a topical nasal decongestant.

### *OCT System*

For our OCT imaging, a specially constructed long-range swept source Fourier domain OCT system was used that has been previously described.<sup>21,22</sup> Rotational scanning of the OCT probe was accomplished using an external rotational motor (Animatics, Santa Clara, CA) coupled to a fiber optic rotary joint (Princetel, Pennington, NJ). Torque from the rotational motor was translated through the coil to the distal probe tip. A dual-motor stage (Zaber Technologies, Vancouver, BC, Canada) allowed for simultaneous linear pullback of the probe toward the nostrils, thus allowing for image acquisition in a helical, retrograde fashion.

### *OCT Imaging*

First, the capability for OCT to reliably measure angles using a standard was demonstrated. This served as a calibration measure. For this purpose, the probe was inserted at different distances within a rectangular metal right angle bracket.

OCT imaging resulted in measurements of 90.5°. However, in cases where the probe was touching/near contact with the apex of the angle bracket and the system offset was not chosen correctly, the OCT images yielded incorrect values. An adjustment in the device software was introduced to compensate for this artifact. This change in the offset value determines the distance of each point in the image from the center of the field. This adjustment to the software does not introduce artifact and is a standard measure with OCT imaging.

OCT imaging of the INV was conducted bilaterally on awake, seated subjects (Fig. 1). Probe rotation and pullback, data acquisition, and real-time image display were controlled by software operating on a Windows platform. OCT probes were encased in a transparent and sterilized fluorinated ethylene propylene sheath (Zeus, Orangeburg, SC). These single-use sheaths were heat-sealed with a butane lighter. With a nasal speculum, the probe was inserted into the nose and advanced on the floor of the nose until the tip of the probe reached the nasopharynx. There, the probe was rotated (25 Hz) and linearly retracted using a servomotor (3.13 mm/s) within the sheath to acquire 3,608 images in a helical fashion with 125- $\mu$ m separation between consecutive frames. Image acquisition started in the nasopharynx and terminated outside the nasal cavity. The sheath was held stationary on the floor of the nose during probe pullback. The subjects held their breath during image acquisition (approximately 15 seconds). Upon completion, the probe and the sheath were removed. Decongestant nasal spray was applied, and after 5 minutes OCT imaging was repeated for both sides. The time to acquire one set of OCT images was approximately 1 minute. Overall procedural time including equipment setup and data acquisition was about 20 minutes.

### *Data Acquisition and Analysis*

Continuous helical scanning from the nasopharynx to the nostril generated about 500 raw images for each OCT data set that were postprocessed into BMP file format (2,000  $\times$  2,048 pixels). Offline data analysis included frame-by-frame examination of OCT data within a graphic viewer (IrfanView; Irfan Skiljan, Wiener Neustadt, Austria). To identify airway anatomy, OCT data were first converted from Cartesian to polar coordinates in MATLAB (MathWorks, Natick, MA). This rendered the data into an anatomic (axial) configuration for ease of visualization and analysis. Levels of the nasal passageway were identified based on distinct topographical characteristics and locations of anatomical structures (e.g., septum and inferior turbinate). The INV was identified by the anterior head of the inferior turbinate and the septum (Fig. 2). It was measured at the most anterior aspect of the turbinate. Seven separate serial images just posterior to the beginning of the inferior turbinate were selected and loaded into Photoshop CC (Adobe Systems, San Jose, CA). Measurements included the angle and the cross-sectional area of the INV (Fig. 2). The angle was measured along the medial and lateral borders of the airway lumen visually averaging the contour irregularities. The area was obtained along the margins of the airway lumen.

The digital endoscopic images were loaded into Photoshop CC, and the angle of the INV was measured in the same way as described above (Fig. 3). For each individual, five different endoscopic pictures for each side and condition were analyzed. The data were not blinded for analysis.

Multiple group comparisons were done using the Kruskal-Wallis test followed by Dunn test. The precision of the applied measuring methods (endoscopy vs. OCT) was assessed by calculating the coefficient of variance (CV) of  $n = 5$  repeated

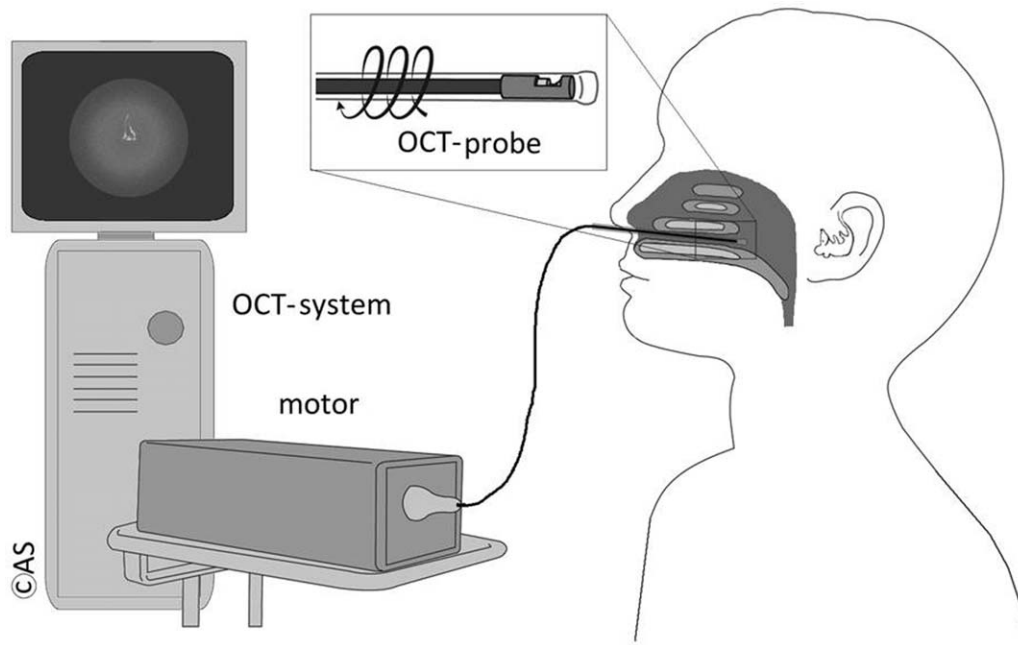


Fig. 1. Optical coherence tomography (OCT) setup. OCT imaging was performed on awake, seated subjects. Probe rotation and pullback, data acquisition, and real-time image display were controlled by Windows-based software. OCT probes were encased in a transparent, single-use, and sterilized fluorinated ethylene propylene sheath.

measurements for both sides in  $n = 32$  cases. Student paired  $t$  test was used to test for differences in mean INV or CV between the two different measuring methods. Differences were considered statistically significant at  $P < .05$ .

## RESULTS

Long-range Fourier domain OCT was performed in 32 nasal airways of 16 healthy subjects. Ten patients were male, and six were female. Eight (five male and three female) subjects were Asian and eight (five male and three female) persons were Caucasian. All 32 cases were performed to completion, without any adverse events.

All 32 data sets demonstrated the gross contour of the nasal airway. The septum and the anterior head of

the inferior turbinate were easily identified in each study.

The INV angle measured by OCT was found to be  $18.3^\circ \pm 3.1^\circ$  (mean  $\pm$  standard deviation [SD]). In the Asian subpopulation, it was found to be  $21.8^\circ \pm 2.9^\circ$  (mean  $\pm$  SD); in the Caucasian subpopulation, it was  $14.2^\circ \pm 3.2^\circ$  (mean  $\pm$  SD). After application of nasal decongestant the INV angle was found to be  $21.7^\circ \pm 3.0^\circ$  (mean  $\pm$  SD), with  $25.2^\circ \pm 3.1^\circ$  (mean  $\pm$  SD) in the Asian and  $18.2^\circ \pm 3.0^\circ$  (mean  $\pm$  SD) in the Caucasian subpopulation; this increase was statistically significant compared to the angle in normal conditions ( $P < .05$ ). The cross-sectional area measured by OCT was  $0.65 \pm 0.23 \text{ cm}^2$  (mean  $\pm$  SD). There was no difference in the cross-sectional area between the Asian and Caucasian

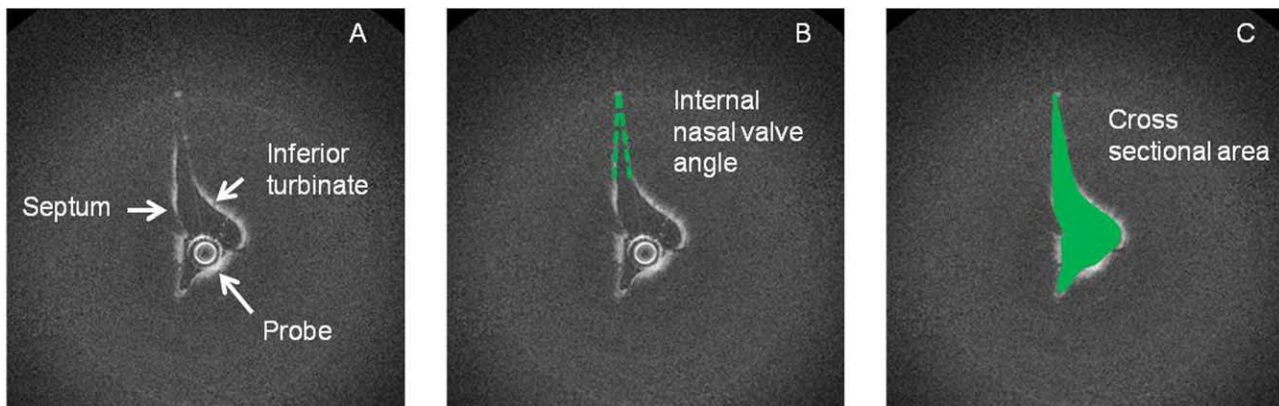


Fig. 2. Optical coherence tomography picture of a left internal nasal valve. (A) The internal nasal valve was identified by the anterior head of the inferior turbinate and the septum. (B) The angle of the internal nasal valve was measured between the septum and the lateral nasal wall. (C) The cross-sectional area was identified. [Color figure can be viewed in the online issue, which is available at [www.laryngoscope.com](http://www.laryngoscope.com).]

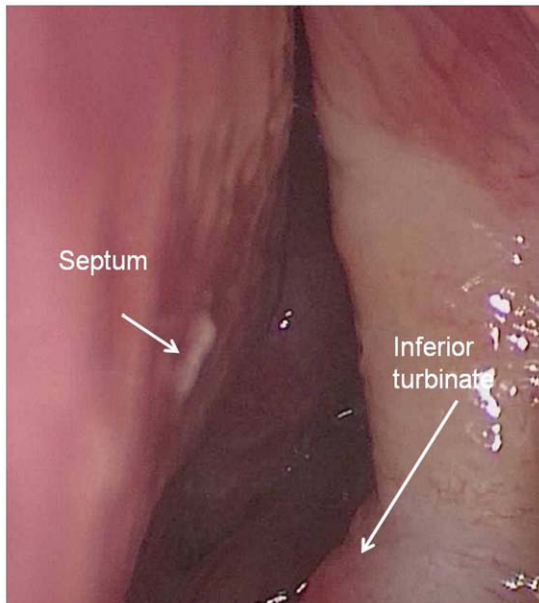


Fig. 3. Endoscopic picture of a left internal nasal valve. [Color figure can be viewed in the online issue, which is available at [www.laryngoscope.com](http://www.laryngoscope.com).]

subpopulations. After application of nasal decongestant, the cross-sectional area was found to be  $0.97 \pm 0.31 \text{ cm}^2$  (mean  $\pm$  SD), which was statistically significant compared to normal conditions ( $P < .05$ ) (Fig. 4).

The INV angle measured by endoscopy was found to be  $18.8^\circ \pm 6.9^\circ$  (mean  $\pm$  SD). After application of nasal decongestant, the INV angle was found to be  $21.7^\circ \pm 6.0^\circ$  (mean  $\pm$  SD), which was statistically significant compared to normal conditions ( $P < .05$ ).

There was no statistically significant difference between endoscopy and OCT in the test result concerning the mean INV angle ( $p = 0.778$ , paired  $t$  test), but there was a significant difference in test precision (CV: 50% vs 15%;  $P < .001$ , paired  $t$  test; Fig 5). For most

subjects, the OCT measurements showed a bimodal clustering of the data. This represents the anatomic difference between the right and the left nasal airway. There was no statistically significant difference between the clusters.

## DISCUSSION

Nasal airway obstruction and the commonly associated reduced quality of life metrics are often caused by incompetence of the INV.<sup>1,3,8,23</sup> It is estimated that about 13% of the general and up to 60% of the geriatric population in the United States have some form of INV malfunction.<sup>24</sup> Methods for diagnosing this condition either are subject to examiner variability, suffer from poor reproducibility, or are very time-consuming. Therefore, it is not surprising that currently, no gold standard test has been defined to diagnose obstruction of the INV.<sup>10</sup>

A recent review and a clinical consensus paper both mentioned history and physical examination as key measures for the examination of the INV. Nasal endoscopy is described to be a possible adjunct test for documentation, whereas radiographic studies are not thought to be useful in evaluating the nasal valve.<sup>3,10</sup> Other objective nasal outcome measures such as rhinomanometry and acoustic rhinometry have several limitations, are not routinely used, and may not be useful for this particular nasal condition.<sup>1,3,10-12</sup>

Because of the frequency of nasal valve malfunction, an objective and reliable test would be of great value for both surgeons and patients. LR-OCT has the capability to accurately delineate the cross-sectional area of hollow organs.<sup>21,22</sup> For this reason, it appears to be a highly suitable method for measuring the cross-sectional area and the angle of the INV.

This is the first report using LR-OCT for the evaluation of nasal valve geometry. In our study, LR-OCT proved to be a relatively fast and easily performed method. It was safe, minimally invasive, and well-

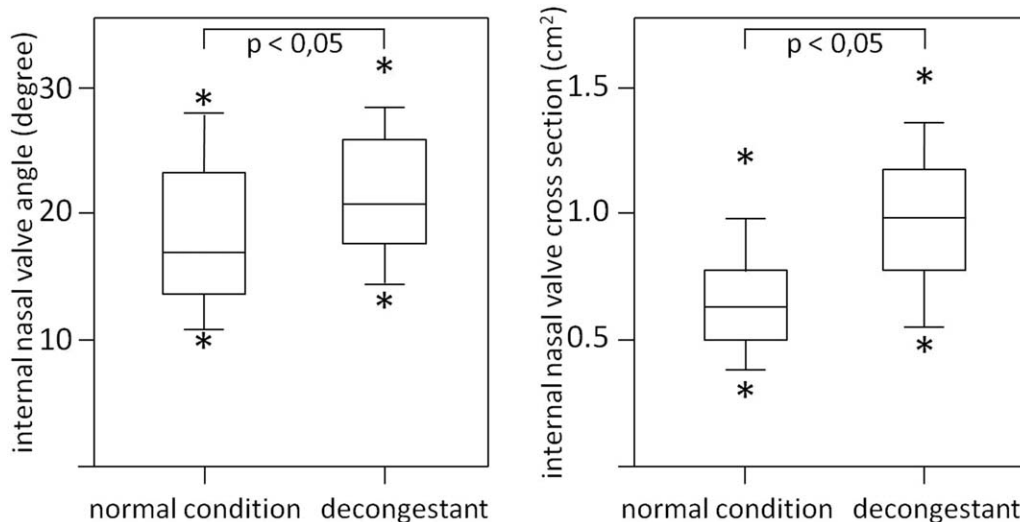


Fig. 4. Internal nasal valve angle (left) and internal nasal valve cross-sectional area (right) measured by optical coherence tomography in normal and decongestant conditions. \*Group comparisons were done using the Kruskal-Wallis test followed by Dunn test.

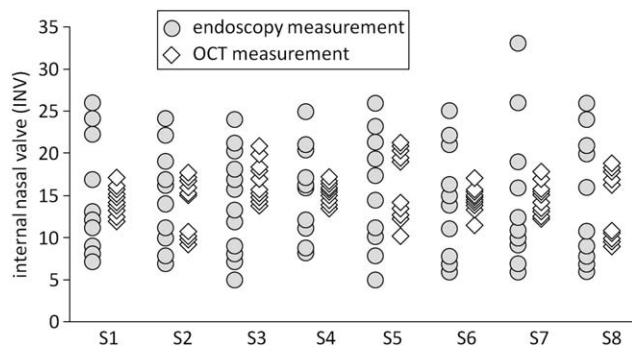


Fig. 5. Internal nasal valve angle measured endoscopically and by optical coherence tomography (OCT) exemplary for eight subjects. The precision of the applied measuring methods was assessed by calculating the coefficient of variance of  $n = 5$  repeated measurements for each side in  $n = 16$  subjects. There was no statistically significant difference between the two methods in the test result regarding the mean angle ( $P = .778$ , paired  $t$  test), but there was a significant difference in test precision ( $P < .001$ , paired  $t$  test).

tolerated in patients without the need for local anesthesia or sedation. With a mean value of  $18.3^\circ$ , the angle of the INV measured by OCT was slightly larger than literature-reported values of  $10^\circ$  to  $15^\circ$ .<sup>2,7,8,14,16</sup> However, these classically described values were collected from a Caucasian population. Only 50% of our study population was Caucasian. With a mean value of  $14.2^\circ$  in the Caucasian population, the angle measured by OCT correlated well with historical ranges of  $10^\circ$  to  $20^\circ$ .<sup>14,16</sup> There are few reports on the measurement of INV area in Asians. A study using CT scans and endoscopy for the measurement of the INV angle in an Asian population reported values of  $21.6^\circ$ ,<sup>17</sup> similar to the mean value of  $21.8^\circ$  in our Asian subpopulation. The cross-sectional area here was found to be  $0.65 \text{ cm}^2$ , correlating well with values estimated using acoustic rhinometry<sup>4-6</sup> ( $0.62\text{--}0.92 \text{ cm}^2$ ,  $0.63 \text{ cm}^2$ , and  $0.73\text{--}0.92 \text{ cm}^2$ ) and CT scans<sup>14,15</sup> ( $0.51$  and  $0.8 \text{ cm}^2$ ). Changes in size could be reliably delineated: analogous to previous studies, LR-OCT here demonstrated an increase in valve angle and cross-sectional area after the application of nasal decongestant.<sup>4-6</sup>

In this study, OCT images were compared to endoscopic digital images, as endoscopy is the only widely accepted adjunct test for examining the nasal valve area.<sup>3,10</sup> Although endoscopy is frequently used for examining the nasal valve area, there are only few studies using endoscopy for measuring the nasal valve angle.<sup>17,25,26</sup> Reasons for the difficulties to obtain objective measurements with endoscopic images might be spherical distortion of the endoscopic optics, varying distances of the endoscopic tip position in each image, and rotation of the endoscope. In our study, the angle of the INV measured by endoscopy was  $18.8^\circ$ , corresponding well to the angle seen with OCT. However, values that were determined by endoscopy showed a significantly higher distribution than the OCT data. The test precision was significantly lower. One possible reason for this spread in the data is that the relative position of the endoscope tip within the nasal airway varied from patient to patient, whereas the OCT probe was kept

stable on the floor of the nose and scanned across the entire valve region. Moreover, estimating the INV angle from endoscopic images was in itself subjective, as it is difficult to identify the precise locus of the lateral wall (Fig. 3). Certainly, there is a measure of subjectivity in estimating valve angle from OCT contours as well, albeit it is substantially less subjective, as OCT provides surface contour information, whereas in a digital image one has to estimate the sidewall location. OCT is not infallible, as mucous, blocked line of sight, and drop-off in signal intensity can reduce image quality.<sup>27</sup>

The objective of this study was to demonstrate the potential use of LR-OCT for performing high-resolution micrometry of the INV region. OCT resolution ( $10 \mu\text{m}$ ) exceeds that of CT ( $1 \text{ mm}$ ) by two orders of magnitude. Future planned studies by our group will focus on determining the value of OCT-measured INV geometry in patients with symptomatic nasal obstruction from valve problems as well as other pathologies. This study is preliminary in nature, and the number of cases is still relatively small. It must be noted that the presented OCT system was specially constructed and is therefore comparatively expensive. Because of the size of the nasal vault and upper airway, no commercially available OCT system can be used in this particular clinical application. There are investigational commercial devices in development, but at this point they are costly. For now, OCT remains an investigational technology used to generate accurate airway models and define airway geometry in vivo.

In the future, we believe that LR-OCT will be a useful tool to evaluate the nasal valve objectively and to provide valuable and precise anatomical information without the risks of ionizing radiation.

Future studies are needed to correlate the LR-OCT with clinical examination findings, patient symptomatology, and disease-specific quality-of-life scores.<sup>9</sup> Also, longitudinal studies should be carried out in which OCT would be used as the primary method to identify patients with nasal airway obstruction caused by incompetence of the INV. Moreover, LR-OCT could be used to evaluate the impact of various nasal valve operations—such as batten and spreader grafts—to increase airway geometry, reduce lateral wall collapse, and increase flow.<sup>28</sup>

## CONCLUSION

This is the first report using long-range LR-OCT for the evaluation of nasal valve geometry. LR-OCT proved to be a relatively fast and easily performed method. OCT could accurately quantify the INV area. The values of the angle and the cross-sectional area of the INV were reproducible and correlated well with the data seen with other methods. Changes in size could be reliably delineated.

Future clinical studies will be necessary to prove the potential of integrating this novel technique into the clinical routine for the pre- and postoperative evaluation of the INV.

## BIBLIOGRAPHY

1. Fattahi T. Internal nasal valve: significance in nasal air flow. *J Oral Maxillofac Surg* 2008;66:1921–1926.

2. Teichgraeber JF, Wainwright DJ. The treatment of nasal valve obstruction. *Plast Reconstr Surg* 1994;93:1174–1182; discussion 1183–1184.
3. Rhee JS, Weaver EM, Park SS, et al. Clinical consensus statement: diagnosis and management of nasal valve compromise. *Otolaryngol Head Neck Surg* 2010;143:48–59.
4. Grymer LF. Reduction rhinoplasty and nasal patency: change in the cross-sectional area of the nose evaluated by acoustic rhinometry. *Laryngoscope* 1995;105(4 pt 1):429–431.
5. Roithmann R, Cole P, Chapnik J, Shpirer I, Hoffstein V, Zamel N. Acoustic rhinometry in the evaluation of nasal obstruction. *Laryngoscope* 1995;105(3 pt 1):275–281.
6. Shaida AM, Kenyon GS. The nasal valves: changes in anatomy and physiology in normal subjects. *Rhinology* 2000;38:7–12.
7. Kasperbauer JL, Kern EB. Nasal valve physiology. Implications in nasal surgery. *Otolaryngol Clin North Am* 1987;20:699–719.
8. Murakami C. Nasal valve collapse. *Ear Nose Throat J* 2004;83:163–164.
9. Rhee JS, Sullivan CD, Frank DO, Kimbell JS, Garcia GJ. A systematic review of patient-reported nasal obstruction scores: defining normative and symptomatic ranges in surgical patients. *JAMA Facial Plast Surg* 2014;16:219–225; quiz 232.
10. Ishii LE, Rhee JS. Are diagnostic tests useful for nasal valve compromise? *Laryngoscope* 2013;123:7–8.
11. Apaydin F. Nasal valve surgery. *Facial Plast Surg* 2011;27:179–191.
12. Fischer H, Gubisch W. Nasal valves—importance and surgical procedures. *Facial Plast Surg* 2006;22:266–280.
13. Hilberg O, Jackson AC, Swift DL, Pedersen OF. Acoustic rhinometry: evaluation of nasal cavity geometry by acoustic reflection. *J Appl Physiol* 1989;66:295–303.
14. Bloom JD, Sridharan S, Hagiwara M, Babb JS, White WM, Constantinides M. Reformatted computed tomography to assess the internal nasal valve and association with physical examination. *Arch Facial Plast Surg* 2012;14:331–335.
15. Moche JA, Cohen JC, Pearlman SJ. Axial computed tomography evaluation of the internal nasal valve correlates with clinical valve narrowing and patient complaint. *Int Forum Allergy Rhinol* 2013;3:592–597.
16. Poetker DM, Rhee JS, Mocan BO, Michel MA. Computed tomography technique for evaluation of the nasal valve. *Arch Facial Plast Surg* 2004;6:240–243.
17. Suh MW, Jin HR, Kim JH. Computed tomography versus nasal endoscopy for the measurement of the internal nasal valve angle in Asians. *Acta Otolaryngol* 2008;128:675–679.
18. Hariri BM, Rhee JS, Garcia GJ. Identifying patients who may benefit from inferior turbinate reduction using computer simulations. *Laryngoscope* 2015.
19. Huang D, Swanson EA, Lin CP, et al. Optical coherence tomography. *Science* 1991;254:1178–1181.
20. Armstrong J, Leigh M, Walton I, et al. In vivo size and shape measurement of the human upper airway using endoscopic longrange optical coherence tomography. *Opt Express* 2003;11:1817–1826.
21. Jing J, Zhang J, Loy AC, Wong BJ, Chen Z. High-speed upper-airway imaging using full-range optical coherence tomography. *J Biomed Opt* 2012;17:110507.
22. Volgger V, Sharma GK, Jing JC, et al. Long-range Fourier domain optical coherence tomography of the pediatric subglottis. *Int J Pediatr Otorhinolaryngol* 2015;79:119–126.
23. Sullivan CD, Garcia GJ, Frank-Ito DO, Kimbell JS, Rhee JS. Perception of better nasal patency correlates with increased mucosal cooling after surgery for nasal obstruction. *Otolaryngol Head Neck Surg* 2014;150:139–147.
24. Hurbis CG. An adjustable, butterfly-design, titanium-expanded polytetrafluoroethylene implant for nasal valve dysfunction: a pilot study. *Arch Facial Plast Surg* 2006;8:98–104.
25. Keck T, Leiacker R, Kuhnemann S, Lindemann J, Rozsasi A, Wantia N. Video-endoscopy and digital image analysis of the nasal valve area. *Eur Arch Otorhinolaryngol* 2006;263:675–679.
26. Miman MC, Deliktas H, Ozturan O, Toplu Y, Akarçay M. Internal nasal valve: revisited with objective facts. *Otolaryngol Head Neck Surg* 2006;134:41–47.
27. Lazarow FB, Ahuja GS, Chin Loy A, et al. Intraoperative long range optical coherence tomography as a novel method of imaging the pediatric upper airway before and after adenotonsillectomy. *Int J Pediatr Otorhinolaryngol* 2015;79:63–70.
28. Frank-Ito DO, Kimbell JS, Laud P, Garcia GJ, Rhee JS. Predicting postsurgery nasal physiology with computational modeling: current challenges and limitations. *Otolaryngol Head Neck Surg* 2014;151:751–759.